

CONF-790125--76

MASTER

## COMPATIBILITY OF MOLTEN SALTS WITH TYPE 316 STAINLESS STEEL AND LITHIUM\*

J. R. KEISER, J. H. DEVAN, AND E. J. LAWRENCE

Oak Ridge National Laboratory, Oak Ridge, Tennessee 37830, USA

Molten salts with possible application in fusion reactors have been studied. The corrosion rate of type 316 stainless steel in  $\text{LiF-BeF}_2$ ,  $\text{KNO}_3\text{-NaNO}_2\text{-NaNO}_3$ , and  $\text{LiF-LiCl-LiBr}$  was strongly affected by the temperature and oxidation potential of the salt. A rapid exothermic reaction occurred when  $\text{KNO}_3\text{-NaNO}_2\text{-NaNO}_3$  was melted with lithium.

### 1. INTRODUCTION

Molten salts are being considered for use in many energy systems, including fusion energy. The possibilities for use of salts in a fusion reactor include the breeding material, the coolant, and a medium to extract tritium from lithium. Of course, potential problems are associated with all these applications. To be suitable for use as a breeding material, it has been noted [1,2] that in addition to breeding a salt would have to permit efficient recovery of tritium, be stable under neutron irradiation and induced electric fields, and be compatible with the containment vessel and any other component the salt might contact. If used as a coolant, a salt must have adequate heat transfer properties, stability under irradiation, and compatibility with materials it might contact. A salt used for extracting tritium from the coolant must have extractability along with compatibility with the containment vessel and the coolant [3]. Since the compatibility requirement is common to all applications, we have studied the compatibility of three salt mixtures with type 316 stainless steel. We have also studied the kinetics of heat release when a potential coolant salt,  $\text{KNO}_3\text{-NaNO}_2\text{-NaNO}_3$ , is mixed with lithium.

### 2. EXPERIMENTAL METHODS

Thermal convection loops (Fig. 1) were used for these metal-salt compatibility studies. They are heated on the bottom and one vertical side. Cooling the other two sides by ambient air causes the molten salt in the tubing to flow at a velocity of about 17 mm/s because of the variation in density of the salt with temperature. Corrosion specimen removal,

\*Research sponsored by the Office of Fusion Energy, U.S. Department of Energy under Contract W-7405-eng-26 with the Union Carbide Corporation.

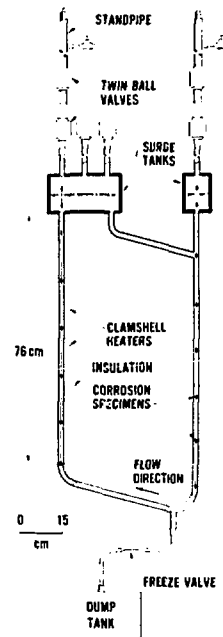


Fig. 1. Schematic Drawing of Thermal Convection Loop.

insertion of electrodes for voltammetry measurements, and material additions to the loop can be made through the surge tanks. Sixteen corrosion specimens were used, eight in the heated vertical leg and eight in the cooled vertical leg. These specimens were removed from the loop every 500 h for weighing and examination. Relative changes in the oxidation potential of the salt and in the concentration of certain impurities and corrosion products were measured on-line by controlled potential voltammetry [2,4]. The measured changes could be correlated with the measured corrosion rates.

#### NOTICE

This report was prepared as an account of work sponsored by the United States Government. Neither the United States nor the United States Department of Energy, nor any of their employees, nor any of their contractors, subcontractors, or their employees, makes any warranty, express or implied, or assumes any legal liability or responsibility for the accuracy, completeness or usefulness of any information, apparatus, product or process disclosed, or represents that its use would not infringe privately owned rights.

REPRODUCTION OF THIS DOCUMENT IS UNLIMITED

Table 1  
Thermal convection loop operating condition

Salt	Loop Material	Specimen Material	Loop Cover Gas	Potential Fusion Reactor Use	Maximum Loop Temperature (°C)	Operation Time (h)	Maximum Temperature Difference (°C)
LiF-BeF <sub>2</sub> (66-37 mol %)	316 stainless steel	316 stainless steel	Ar	Blanket, coolant	650	25,193	125
KNO <sub>3</sub> -NaNO <sub>2</sub> -NaNO <sub>3</sub> (44-49-7 mol %)	Hastelloy N	316 stainless steel and Hastelloy N	N <sub>2</sub>	Coolant	430 505 550	5,472 7,032 8,400	70 80 90
LiF-LiCl-LiBr (22-31-47 mol %)	316 stainless steel	316 stainless steel	Ar	Extraction of tritium from lithium	530	2,618	60

The three loop experiments used the salts, materials, and conditions listed in Table 1. All incorporate removable specimens and controlled potential voltammetry.

In addition to the corrosion experiments, we studied the reactions between lithium and KNO<sub>3</sub>-NaNO<sub>2</sub>-NaNO<sub>3</sub>. We heated a sealed capsule containing 0.3 g Li and 10 g salt while monitoring the temperature with thermocouples and the pressure with a transducer. After completion of the experiment, the gaseous and solid contents of the capsule were analyzed.

### 3. CORROSION STUDIES OF LiF-BeF<sub>2</sub>

We conducted a relatively long-term closed loop test of type 316 stainless steel with the salt LiF-34 mol % BeF<sub>2</sub>. The corrosion rates reflect normally occurring redox reactions, which result in mass transfer of corrosion products from hot to cold regions of the loop. The maximum hot-leg temperature was 650°C; other operating conditions are listed in Table 1.

The effect of time on corrosion at the hottest point in this loop is indicated by the lower curve in Fig. 2. The corrosion rate was relatively rapid during the first 1000 h, then decreased substantially over the next 1000 h, and decreased more slowly thereafter. The rate between 3000 and 9000 h averaged 8 μm/year.

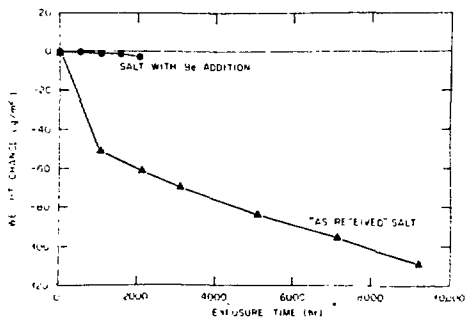


Fig. 2. Weight change versus exposure time for type 316 stainless steel in LiF-BeF<sub>2</sub> salt at the maximum loop temperature of 650°C.

During the first 3000 h of operation with the as-received salt, the chromium concentration increased from 40 to about 400 wt ppm, while iron and nickel concentrations remained nearly constant. The weight loss from the corrosion specimens is primarily due to loss of chromium.

The upper curve in Fig. 2 shows the corrosion rate of type 316 stainless steel in the same loop but with beryllium metal added to the salt [2]. The beryllium addition reduced the corrosion rate to less than 2 μm/year over the 2000-h test period. The effect of the beryllium was also evident in the voltammetric measurements. The limit potential of the salt decreased as soon as the beryllium was added and then gradually increased to its former value as the beryllium was oxidized to BeF<sub>2</sub>.

The results show that the corrosion rate of type 316 stainless steel can be reduced to a negligible level by addition of a metallic reductant such as beryllium to the LiF-BeF<sub>2</sub> salt. In the absence of a reductant the corrosion rate decreases monotonically with time. However, the level remains higher than with the reductant even after nearly 10,000 h.

### 4. CORROSION STUDIES OF LiF-LiCl-LiBr

The corrosion properties of the LiF-LiCl-LiBr tritium extraction salt in a type 316 stainless steel thermal convection loop were determined. Operating conditions of this loop are given in Table 1. Chemical analysis of the as-received electrochemically purified salt,\* as well as on-line voltammetric measurements, indicate very low impurity levels. Specimens of type 316 stainless steel have been exposed to the as-received salt at a maximum temperature of 530°C for a total of almost 2700 h. Weight changes measured during this time were very small. All specimens showed a nearly linear weight loss during 2000 h operation. The maximum calculated corrosion rate is only 2 μm/year. Voltammetry measurements on this salt show that impurities introduced when the specimens were inserted caused perturbation in the limit potential that decayed in about 15 d.

\*Furnished by V. Maroni of Argonne National Laboratory.

## 5. CORROSION STUDIES OF $\text{KNO}_3\text{-NaNO}_2\text{-NaNO}_3$

A possible low-melting coolant is the eutectic salt mixture of  $\text{KNO}_3\text{-NaNO}_2\text{-NaNO}_3$ , with a melting point of  $142^\circ\text{C}$  ( $288^\circ\text{F}$ ). Corrosion in this salt has been measured as a function of loop operating temperature and specimen composition. Table 1 gives the loop operating conditions. Weight changes that occurred during exposure [Fig. 3(a)] indicate that corrosion of type 316 stainless steel increased with temperature. The corrosion rate at the hottest point when the loop operated with a maximum temperature of  $430^\circ\text{C}$  was  $7 \mu\text{m}/\text{year}$ , and the rate was  $8 \mu\text{m}/\text{year}$  for a maximum temperature of  $505^\circ\text{C}$ . All type 316 stainless specimens had a dark oxide surface layer. Electron microprobe examination on the coating found on the hottest specimen indicated that the outer oxide layer is low in iron compared with the bulk, while the metallic components of the inner layer are in about the same proportions as in the alloy. Electron microprobe analysis of the layers found on the coolest specimen revealed that the outer region was rich in nickel and depleted in chromium, while the inner layer was high in iron and nickel and very low in chromium. The oxide observed on all specimens was fairly adherent but apparently had some solubility in the salt.

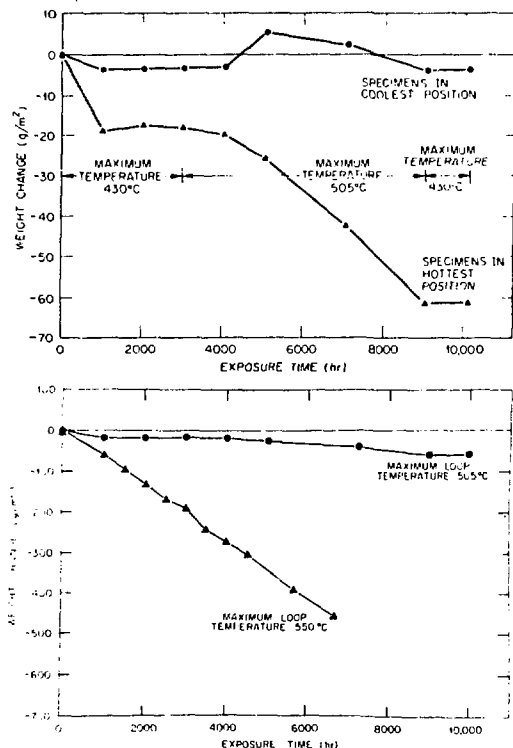


Fig. 3. Weight change versus exposure time for type 316 stainless steel in  $\text{KNO}_3\text{-NaNO}_2\text{-NaNO}_3$ . (a) Run at 430 and  $505^\circ\text{C}$ . (b) Run at  $550^\circ\text{C}$ .

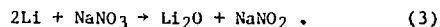
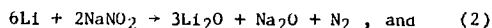
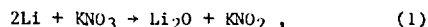
The weight change data obtained on the hottest specimen during operation of the loop with a  $550^\circ\text{C}$  maximum temperature is shown in Fig. 3(b). Included in this graph is the lower temperature data as a reference. Clearly, a significantly higher weight loss occurred when the system was operated at  $550^\circ\text{C}$ . For operation at  $550^\circ\text{C}$  peak, in some cases a greater weight loss was observed at intermediate temperatures (about  $520^\circ\text{C}$ ) than at the maximum temperature. The calculated corrosion rate at the maximum temperature was  $74 \mu\text{m}/\text{year}$ .

Two specimens of Hastelloy N, a nickel-base 7% Cr alloy, were also exposed in this loop. Hastelloy N lost less weight for comparable conditions than did type 316 stainless steel. Calculated corrosion rates for Hastelloy N are included in Table 2 along with the calculated corrosion rates for other salt-metal combinations.

Chemical analysis of the salt has been used to help explain the corrosion in these thermal convection loops. Concentrations of Fe, Ni, and Cr in the nitrate-nitrite salt are shown in Table 3. The data show that iron and nickel concentrations in the salt decreased during operation at  $505^\circ\text{C}$  and below. During operation at  $550^\circ\text{C}$ , the concentration of the two elements increased. The concentration of chromium in the salt continually increased for all operating conditions; the greatest increases were during the highest temperature operation. Determination of Cr (VI) showed that only about 5% of the chromium in the salt was in the +6 oxidation state. From these chemical analyses we can conclude that chromium plays a major role in corrosion of the type 316 stainless steel, but the chromium will be in the +2 or +3 oxidation state and not in the highly oxidized +6 state.

## 6. MIXING STUDIES OF $\text{KNO}_3\text{-NaNO}_2\text{-NaNO}_3$ WITH LITHIUM

An area of concern in the use of  $\text{KNO}_3\text{-NaNO}_2\text{-NaNO}_3$  coolant salt is the reaction that might occur if the salt comes in contact with liquid lithium breeding material. The reactions that might occur are:



Another oxide of lithium,  $\text{LiO}_2$ , exists, but its formation is not expected in the presence of Li,  $\text{NaNO}_2$ , or  $\text{KNO}_2$ . Thermodynamic calculations based on room-temperature heats of formation indicate that reactions (2) and (3) are the more probable.

The first heating experiment with these salts revealed that a rapid exothermic reaction occurred near  $200^\circ\text{C}$ . A more carefully monitored second run gave the results shown in Table 4. Quite likely the reaction started when the lithium melted and became available to mix with the salts. Concurrent with the temperature

Table 2  
Calculated corrosion rates for specimen at maximum temperature<sup>1</sup>

Salt	Maximum Temperature (°C)	Condition of Salt	Specimen Material	Loss (µm/year)
LiF-BeF <sub>2</sub>	650	As received	316 stainless steel	15
LiF-BeF <sub>2</sub>	650	After Be addition	316 stainless steel	2
KNO <sub>3</sub> -NaNO <sub>2</sub> -NaNO <sub>3</sub>	430	As received	316 stainless steel	7
			Hastelloy N	3
KNO <sub>3</sub> -NaNO <sub>2</sub> -NaNO <sub>3</sub>	505	As received	316 stainless steel	8
			Hastelloy N	5
KNO <sub>3</sub> -NaNO <sub>2</sub> -NaNO <sub>3</sub>	550	As received	316 stainless steel	7
			Hastelloy N	7
LiF-LiCl-LiBr	530	As received	316 stainless steel	2

<sup>1</sup>The calculations assume that material is removed uniformly from the surface.

<sup>2</sup>Specimens at intermediate temperatures showed rates up to 140 µm/year.

Table 3  
Accumulation of corrosion products in KNO<sub>3</sub>-NaNO<sub>2</sub>-NaNO<sub>3</sub> in Hastelloy N loop<sup>a</sup>

Sample Number	Total Operating Time (h)	Maximum Loop Temperature (°C)	Concentration, ppm		
			Cr	Fe	Ni
	0		200	200	99
1	1,512	430	92	17	12
2	2,832	430	70	10	8
3	5,368	505	93	7	2
4	9,072	505	163	1	0.1
5	13,632	550	303	34	9
6	15,150	550	429	25	16
7	16,440	550	555	131	27
8	21,120	550	747		

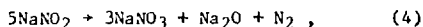
<sup>a</sup>The concentrations probably represent dissolution of the stainless steel specimens, since the Hastelloy N loop material corrodes at a much lower rate and contains less chromium.

Table 4  
Measurements during continuous heating of mixed lithium and KNO<sub>3</sub>-NaNO<sub>2</sub>-NaNO<sub>3</sub><sup>a</sup>

Measurement Location	Temperature, °C		Time to Reach Maximum Temperature (min)
	Reaction Start	Maximum	
Thermocouple well	163	299	<1
Capsule outer surface	177	201	7

<sup>a</sup>Salt mixture melting point 142°C, Li melting point 179°C.

increase, the pressure increased from 0.13 to 0.22 MPa (19 to 32 psi). Subsequent analysis of a gas sample indicated that some nitrogen had been released, and x-ray analysis of the solid residue in the capsule indicated that Li<sub>2</sub>O had also been produced. The evidence seems to favor reaction (2); however, the thermal decomposition reaction,



is known to occur at temperatures above 400°C and has to be considered as a possible source of the nitrogen.

This study shows that molten lithium and KNO<sub>3</sub>-NaNO<sub>2</sub>-NaNO<sub>3</sub> undergo a rapid, exothermic reaction with production of Li<sub>2</sub>O and N<sub>2</sub>. No evidence of

a reaction between solid lithium and the molten salt was observed under these conditions.

## 7. SUMMARY

This work has shown the effect of salt oxidation potential, maximum operating temperature, and alloy composition on the compatibility of alloys with molten salts. In particular, the reduction of the corrosion rate by an addition of beryllium to LiF-BeF<sub>2</sub> demonstrates a means to control corrosion when tritium is being bred in this salt. This work has also shown that the corrosion rate of type 316 stainless steel by the KNO<sub>3</sub>-NaNO<sub>2</sub>-NaNO<sub>3</sub> salt mixture is very much a function of temperature. As a result, it appears this alloy should not be used at or above 550°C in the nitrate-nitrite salt unless a high corrosion rate can be tolerated. An alternative, if this salt must be used at or above 550°C, is to use a more corrosion-resistant alloy such as Hastelloy N.

Mixing of liquid lithium with molten KNO<sub>3</sub>-NaNO<sub>2</sub>-NaNO<sub>3</sub> gave a rapid, exothermic reaction, which indicates a potential problem for a fusion reactor using a lithium blanket and nitrate-nitrite salt coolant.

## REFERENCES

- [1] W. R. Grimes and S. Cantor, "Molten Salt Blanket Fluids in Controlled Fusion Reactors," *The Chemistry of Fusion Technology*, D. M. Gruen, ed., (Plenum Press, New York, 1972), p. 161.
- [2] J. R. Keiser, J. H. DeVan, and D. L. Manning, *The Corrosion Resistance of Type 316 Stainless Steel to Li<sub>2</sub>BeF<sub>4</sub>*, ORNL/TM-5782 (1977), Oak Ridge National Laboratory Report.
- [3] W. F. Calaway, *Nucl. Technol.* 39 (1978).
- [4] J. R. Keiser, *Compatibility Studies of Potential Molten-Salt Breeder Reactor Materials in Molten Fluoride Salts*, ORNL/TM-5783 (1977), Oak Ridge National Laboratory Report.